THE JOURNAL OF BIOLOGICAL CHEMISTRY VOL. 286, NO. 10, pp. 8655–8665, March 11, 2011

Klotho Inhibits Transforming Growth Factor-β1 (TGF-β1) Signaling and Suppresses Renal Fibrosis and Cancer Metastasis in Mice*[S]

Received for publication, August 10, 2010, and in revised form, January 4, 2011 Published, JBC Papers in Press, January 5, 2011, DOI 10.1074/jbc.M110.174037

Shigehiro Doi[‡1], Yonglong Zou[§1], Osamu Togao[¶], Johanne V. Pastor[‡], George B. John[‡], Lei Wang[‡], Kazuhiro Shiizaki[‡], Russell Gotschall[‖], Susan Schiavi[‖], Noriaki Yorioka[**], Masaya Takahashi[¶], David A. Boothman[§2], and Makoto Kuro-o[‡3]

*From the Departments of [‡]Pathology, [§]Oncology, and [¶]Advanced Imaging Research Center, University of Texas Southwestern Medical Center, Dallas, Texas 75390, the [‖]Genzyme Corporation, Cambridge, Massachusetts 02142, and the **Department of Advanced Nephrology, Graduate School of Biomedical Sciences, 1-2-3 Kasumi, Minami-ku, Hiroshima-shi, Hiroshima 734-8551, Japan*

Fibrosis is a pathological process characterized by infiltration and proliferation of mesenchymal cells in interstitial space. A substantial portion of these cells is derived from residing non-epithelial and/or epithelial cells that have acquired the ability to migrate and proliferate. The mesenchymal transition is also observed in cancer cells to confer the ability to metastasize. Here, we show that renal fibrosis induced by unilateral ureteral obstruction and metastasis of human cancer xenografts are suppressed by administration of secreted Klotho protein to mice. Klotho is a single-pass transmembrane protein expressed in renal tubular epithelial cells. The extracellular domain of Klotho is secreted by ectodomain shedding. Secreted Klotho protein directly binds to the type-II TGF-β receptor and inhibits TGF-β1 binding to cell surface receptors, thereby inhibiting TGF-β1 signaling. Klotho suppresses TGF-β1-induced epithelial-to-mesenchymal transition (EMT) responses in cultured cells, including decreased epithelial marker expression, increased mesenchymal marker expression, and/or increased cell migration. In addition to TGF-β1 signaling, secreted Klotho has been shown to inhibit Wnt and IGF-1 signaling that can promote EMT. These results have raised the possibility that secreted Klotho may function as an endogenous anti-EMT factor by inhibiting multiple growth factor signaling pathways simultaneously.

The *klotho* gene was originally identified as a putative aging-suppressor gene in mice that extended life span when overexpressed (1) and induced complex phenotypes resembling human premature-aging syndromes when disrupted (2). The *klotho* gene belongs to a family 1 glycosidases and encodes a single-pass transmembrane protein of ~135 kDa expressed predominantly in renal tubular epithelial cells (2). The intracellular domain is very short (10-amino acid long) and has no known functional domains. The extracellular domain is subject to ectodomain shedding. Klotho protein is clipped on the cell surface by membrane-anchored proteases and the entire extracellular domain (~130 kDa) is released into systemic circulation (1, 3–5). Thus, Klotho protein exists in two forms: membrane Klotho and secreted Klotho.

Membrane Klotho functions as an obligate co-receptor for fibroblast growth factor-23 (FGF23) (6, 7). FGF23 is a bone-derived hormone that acts on kidney to promote phosphate excretion into urine and suppress vitamin D synthesis, thereby inducing negative phosphate balance (8, 9). One critical feature of FGF23 is that it has very low affinity to FGF receptors (10). FGF23 requires membrane Klotho to bind to its cognate FGF receptors and exert its biological activity. Membrane Klotho forms a constitutive binary complex with FGF receptors to create a *de novo* high-affinity binding site for FGF23 (6, 11). Namely, membrane Klotho functions as an obligate co-receptor for FGF23.

Secreted Klotho functions as a humoral factor independently of FGF23. Secreted Klotho regulates activity of multiple ion channels (12–14) and transporters (15) on the cell surface by modifying their *N*-linked glycans through its putative glycosidase activity. In addition, secreted Klotho binds to Wnt ligands (16) and receptors for insulin/IGF-1 (1, 17) to inhibit signaling mediated by these growth factors.

Transgenic mice that overexpress Klotho are resistant to renal fibrosis caused by chronic glomerulonephritis (18). Renal fibrosis is characterized by infiltration and proliferation of myofibroblasts (fibroblast-like mesenchymal cells with contractile capability) in interstitial space. The origin of myofibroblasts can be fibroblasts migrating from bone marrow (19), residing renal proximal tubular cells (19), and/or renal interstitial pericytes (20). Regardless of the origin, these cells must

* This work was supported, in whole or in part by Grants R01AG019712 (to M. K.), R01CA102792 (to D. A. B.), R01CA129011 (to M. T.), and R21EB009147 (to M. T.) from the National Institutes of Health. This work was also supported by the Dept. of Energy (DE-FG02-09ER64789, to D. A. B.), Genzyme (Genzyme Renal Innovations Program, to M. K.), and Philips Japan (Cooperative Research Grant, to M. T.). R. G. and S. S. are employees of Genzyme Corporation.

[S] The on-line version of this article (available at http://www.jbc.org) contains supplemental Figs. S1–S6 and Table S1.

[1] Both authors contributed equally to this work.

[2] To whom correspondence may be addressed: Dept. of Oncology, University of Texas Southwestern Medical Center at Dallas, 5323 Harry Hines Blvd., Dallas, TX 75390-8807. Tel.: 214-645-6371; Fax: 214-645-6347; E-mail: david.boothman@utsouthwestern.edu.

[3] To whom correspondence may be addressed: Departments of Pathology, University of Texas Southwestern Medical Center at Dallas, 5323 Harry Hines Blvd., Dallas, TX 75390-9072. Tel.: 214-648-4018; Fax: 214-648-4033; E-mail: makoto.kuro-o@utsouthwestern.edu.

undergo a phenotypic transition and acquire the ability to migrate and proliferate to become myofibroblasts. This cellular process (mesenchymal transition) is regarded as a response to tissue injury, but can result in fibrosis under pathological settings in kidney as well as in many other tissues, including liver, lung, and heart (21). Importantly, cancer cells can also undergo mesenchymal transition and acquire the ability to migrate and proliferate, leading to metastasis (21).

Although several cytokines and growth factors are involved in mesenchymal transition, TGF-β1 has been identified as the most potent and universal growth factor that can independently induce mesenchymal transition in various types of cells (22). TGF-β1 inhibits expression of the genes essential for an epithelial phenotype (*e.g.* E-cadherin) and induces expression of the genes that confer a mesenchymal phenotype (*e.g.* vimentin, collagen-1, N-cadherin) and invasiveness (*e.g.* metalloproteases), thereby conferring the ability to migrate on the cell (23). The critical role of TGF-β1 in tissue fibrosis and cancer metastasis has been further endorsed by the fact that neutralizing antibodies for TGF-β1 suppress renal fibrosis (24, 25) and cancer metastasis (26).

In this work, we report a novel function of secreted Klotho; it interferes TGF-β1 signaling by directly binding to type-II TGF-β receptor and inhibiting TGF-β1 binding. We also show that renal fibrosis is associated with significant decrease in renal Klotho expression and that Klotho replacement therapy (injection of secreted Klotho protein) alleviates renal fibrosis. Lastly, we show that secreted Klotho protein inhibits EMT in cultured cancer cells and suppresses cancer metastasis in mice.

EXPERIMENTAL PROCEDURES

Mice—Klotho-overexpressing transgenic mice (*EFmKL46*) and their wild-type controls were previously described (1, 2). All the other mice were purchased from The Jackson Laboratories (Bar Harbor, ME). All animal experiments were approved by the Institutional Animal Care and Use Committee at the University of Texas Southwestern Medical Center at Dallas.

Generation of Recombinant Klotho Protein—A pcDNA3.1 expression vector containing cDNA encoding the rat Klotho extracellular domain (Met^{1} to Lys^{990}) with an HPC4 tag (EDQVDPRLIDGK) attached to the C terminus was stably transfected in CHO-K1 cells. Recombinant rat secreted Klotho protein was purified from conditioned medium by anti-HPC4 monoclonal antibody affinity chromatography followed by Superdex 200 chromatography.

Unilateral Ureteral Obstruction (UUO)—Under general anesthesia, mice (129S1/SvImJ males, 8 weeks of age) were subjected to unilateral ureteral obstruction (UUO)[4]: the right ureter is exposed after a midline abdominal incision and double-ligated. Immediately after surgery, mice were administered with secreted Klotho protein (0.01 mg/kg or 0.02 mg/kg in 0.1 ml of vehicle), vehicle (0.1 ml of 50 mM HEPES, 150 mM NaCl, 3 μM DTT, 0.00003% Tween 80, pH 7.4), neutralizing anti-TGF-β1 antibody (1D11, 1.5 mg/kg, R&D Systems, Minneapolis, MN), or normal mouse IgG_1 (1.5 mg/kg, R&D Systems) by intraperitoneal injection. The same treatments were repeated every 48 h until mice were used 3 or 7 days after UUO surgery.

Magnetic Resonance Imaging (MRI)—T2-weighed images and ADC maps were generated using a 7-T small-animal MR system (Varian, Palo Alto, CA) as previously described (27).

Histological Analysis—Kidneys were excised before or 3 or 7 days after UUO. A part of the kidney was fixed in buffered 10% formalin and processed for standard paraffin sections. The sections were stained with hematoxylin-eosin for cell density measurement as previously described (27). The sections were also stained with Masson's trichrome to detect fibrotic area as blue staining, which was quantified by manually tracing the blue area in 5 randomly selected microscopic fields as in cell density measurements.

Immunohistochemistry—Paraffin sections of the kidney were stained with antibodies against αSMA (Sigma) and collagen-1 (Abcam, Cambridge, MA) as previously described (28). The signal intensity of collagen-1 was quantified using ImageJ software as previously described (28).

Cell Culture and Transfection—Rat renal epithelial (NRK52E) and human embryonic kidney (HEK293) cells were obtained from the American Type Culture Collection (ATCC, Manassas, VA). A549 and 3LL (Lewis Lung cancer) cells were generous gifts from Drs. John Minna and Philip Thorpe at UT Southwestern, respectively. These cells were maintained in Dulbecco's modified Eagle's medium (DMEM) containing 5% or 10% fetal bovine serum (FBS) and penicillin/streptomycin. The A549 cell line that stably expressed Klotho (A549KL) and the control line (A549mock) were generated by transfecting a Klotho expression vector (pEFmKL) (6) or empty vector (pEF1, Invitrogen, Carlsbad, CA), respectively, followed by G418 selection as previously described (6). All cells were mycoplasma-free.

Luciferase Reporter Assay—HEK293 and A549 cells were transfected with a reporter vector that expressed luciferase under the control of Smad (pGTCT2 × 2-Luc) and a lacZ expression vector for normalization using Lipofectamine (Invitrogen). Sixteen (16) hours after transfection, medium was changed to DMEM with 0.05% FBS and, 2 h later inoculated with Klotho or vehicle. Fifteen (15) minutes later cells were stimulated with TGF-β1 (1.0 ng/ml) for 24 h and subjected to standard luciferase and β-galactosidase assays.

Quantitative RT-PCR (qPCR)—RNA extraction and qPCR were performed as previously described (6, 29). Primers used for qPCR were shown in supplemental Table S1.

Immunoblot Analysis—Protein extraction and immunoblot analysis were performed as previously described (6, 29). Primary antibodies used in this study were Klotho (KM2119)(30), αSMA, Vimentin (Santa Cruz Biotechnology), E-Cadherin (BD Biosciences, San Jose, CA), N-cadherin (Santa Cruz Biotechnology), phosphorylated Smad2 (Cell Signaling Technology, Beverley, CA), phosphorylated Smad3 (Cell Signaling), Smad2 (Cell Signaling), Smad3 (Cell Signaling), GAPDH (Abcam). Secondary antibodies used in this study were mouse IgG-HRP, rat IgG-HRP, and human IgG-HRP (GE Healthcare, UK). Signals were detected using the SuperSignal West Dura system (Thermo Fisher, Rockford, IL).

[4] The abbreviations used are: UUO, unilateral ureteral obstruction; EMT, epithelial-to-mesenchymal transition; ADC, apparent diffusion coefficient; SMA, smooth muscle actin.

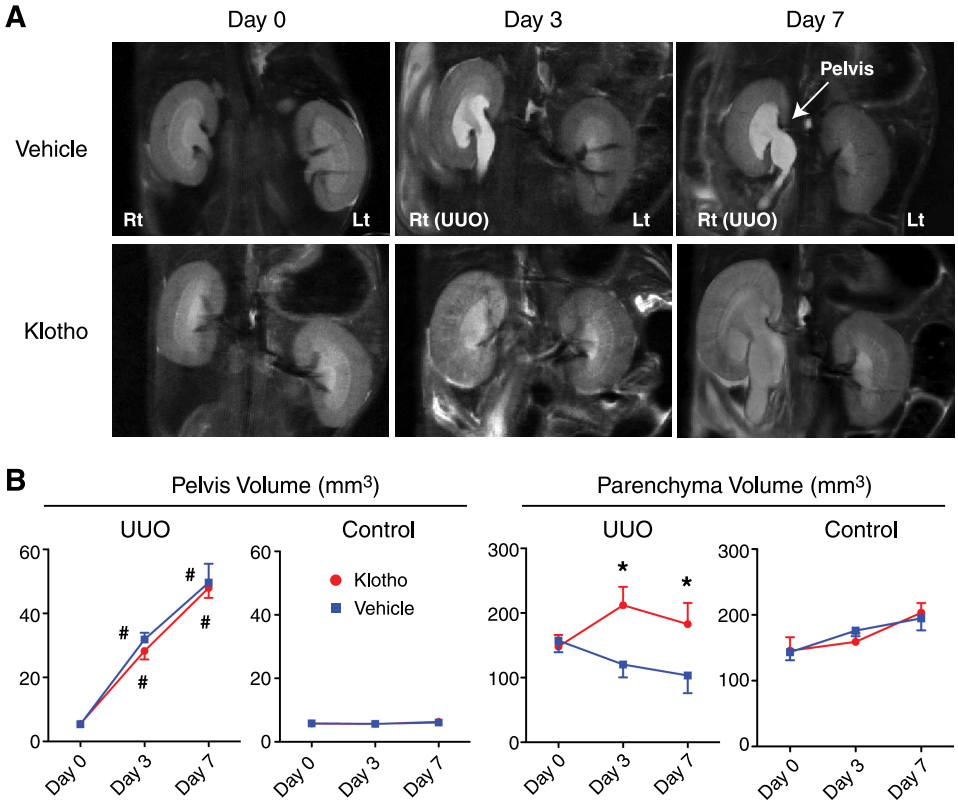

FIGURE 1. **Effects of Klotho protein injection on renal morphology in UUO mice determined by MRI.** *A*, typical T2 weighted MR images from mice before (Day 0) and after UUO (Day 3 and Day 7) administered with vehicle (*upper panels*) or Klotho (0.02 mg/kg, *lower panels*) by intraperitoneal injection every 48 h. The *arrow* indicates enlarged pelvis. *B*, changes in the volume of pelvis and parenchyma determined by the MR images. Right kidneys (UUO) and left kidneys (Control) from Klotho-treated mice (*red*, $n = 6$) and vehicle-treated mice (*blue*, $n = 4$) were compared.

Klotho Binding Assay in Vitro—Recombinant proteins of receptor ectodomain (TGFβR1, TGFβR2, FGFR1c, FGFR1b, LRP6, EGFR, PDGFR) with an Fc tag on the C termini (1 μg, R&D Systems) were incubated with Protein A-Sepharose beads (20 μl of 50% v/v slurry, Thermo Fisher) in 0.2 ml of binding buffer (Krebs-Ringer-Hepes buffer (KRH) with 0.1% bovine serum albumin (BSA)) at room temperature for 1 h. After washing with binding buffer, Klotho protein (0.66 μg in 0.2 ml of binding buffer) was added and incubated at room temperature for 1 h. The beads were washed three times with binding buffer and three times with KRH without BSA. The beads were then boiled in SDS-sample loading buffer and subjected to immunoblot analyses using anti-Klotho (KM2119) or anti-human IgG-HRP (GE Healthcare) antibodies. To determine the apparent dissociation constant (K_d) between Klotho and TGFβR2 *in vitro*, quantitative binding assay was performed. Recombinant TGFβR2 ectodomain with an Fc tag (2.5 ng) was incubated with protein A beads (20 μl of 50% v/v slurry) in 0.2 ml of binding buffer. After washing, the beads were resuspended in 0.2 ml of binding buffer containing Klotho protein (0.3 nM) and incubated at room temperature for 1 h. The supernatant and the beads were separated by centrifugation. Concentration of bound Klotho and free Klotho was quantified by immunoblot analyses using known amounts of recombinant Klotho protein for calibration. Nonspecific binding (Klotho binding to protein A beads without TGFβR2) was undetectable by immunoblot analysis. The K_d was calculated using Equation 1.

$$K_d = [\text{free Klotho}]([\text{total TGF}\beta\text{R2}] - [\text{bound Klotho}])/[\text{bound Klotho}] \quad \text{(Eq. 1)}$$

TGF-β1 Binding Assay in Vitro—Recombinant TGFβR2 (2.5 ng) was incubated with protein A beads (20 μl of 50% v/v slurry) in 0.2 ml of binding buffer (KRH with 0.1% BSA) for 1 h at room temperature. After washing, the beads were incubated in 0.2 ml of binding buffer containing a fixed amount of ^{125}I-TGF-β1 (0.25 nM) and increasing amount of Klotho (0–8.3 nM) for 1 h at room temperature. Beads were washed three times with KRH with 0.1% BSA, three times with KRH without BSA, and then counted in a scintillation counter. Nonspecific binding was determined by replacing Klotho with unlabeled TGF-β1 in excess of 100-fold of ^{125}I-TGF-β1. The K_d between TGF-β1 and TGFβR2 *in vitro* (0.77 nM) was calculated based on the count from samples without Klotho. The equilibrium dissociation constant of Klotho calculated by the allosteric modulator model and by the one-site fit model (the Prism 5 software) was 3.5 and 3.4 nM, respectively.

Inhibition of TGF-β1 Binding in Cultured Cells—NRK52E and A549 cells were cultured to confluence in 24-well plates. Wells were washed with KRH with 0.1% BSA and then incubated for 1 h at room temperature with a fixed amount of ^{125}I-TGF-β1 (0.25 nM) and increasing amount of Klotho (0, 0.1, and

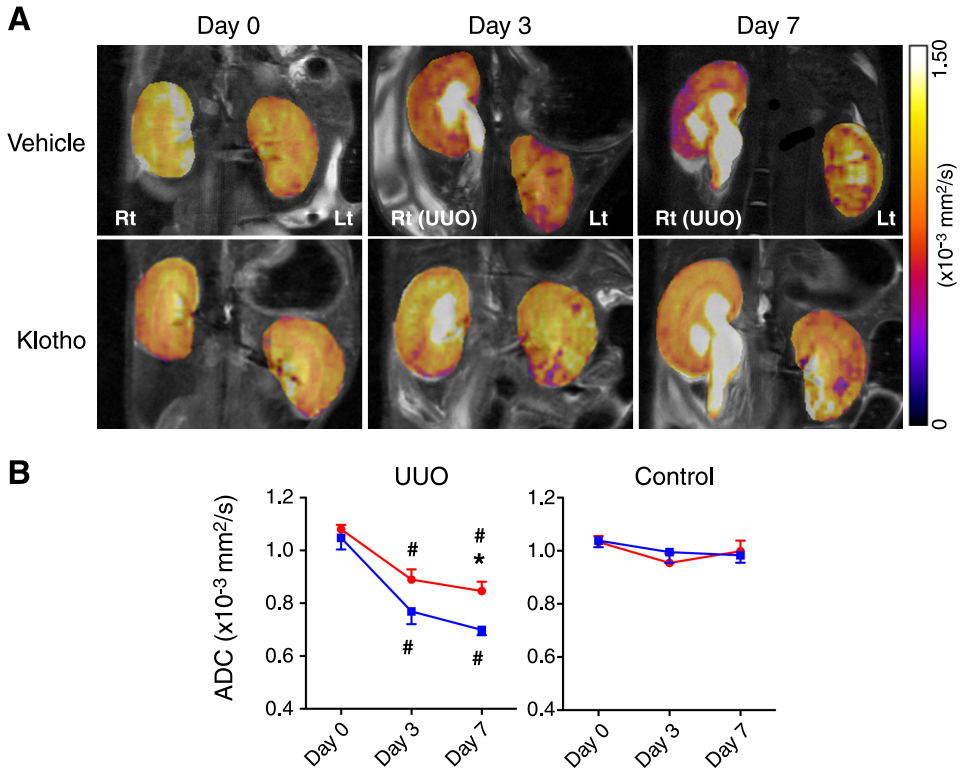

FIGURE 2. **Effects of Klotho protein injection on renal cell density in UUO mice determined by MRI.** *A*, typical ADC maps from mice before (Day 0) and after UUO (Day 3 and Day 7) administered with vehicle (*upper panels*) or Klotho (0.02 mg/kg, *lower panels*). *B*, changes in the average ADC values. Data indicate means ± S.E. *, $p < 0.05$ *versus* vehicle-treated mice at the same time points by two-tailed *t* test. #, $p < 0.05$ *versus* mice at Day 0 by two-tailed *t* test.

0.3 nM). The cells were rinsed three times with ice-cold KRH with 0.1% BSA, lysed in 0.2 ml of lysis buffer (1% SDS and 1N NaOH), and counted in a scintillation counter. Nonspecific binding was determined by replacing Klotho with unlabeled TGF-β1 at 100-fold of ^{125}I-TGF-β1.

Cancer Cell Transplantation—A549mock or A549KL cells were injected into athymic mice (females at 8 weeks of age) by tail vein injection (2×10^6 cells per mouse). 3LL cells were injected into wild-type mice (8 weeks of age) and age/sex-matched Klotho-overexpressing transgenic mice (2×10^6 cells per mouse) by tail vein injection. Also, 3LL cells were injected into wild-type mice (2×10^6 cells per mouse, 8 weeks of age) and then treated with either Klotho protein (0.01 mg/kg, intraperitoneal) or vehicle every other day. Survival of mice was monitored for Kaplan-Meier analyses. For quantification of metastasis, A549mock and A549KL cells were labeled with GFP and RFP, respectively, and mixed at 1:1 ratio. Mixed A549 cells were injected into athymic mice (2×10^6 cells per mouse). Lungs were harvested 7 days after injection, digested with collagenase I, and plated on 10 cm plates for 9 days. Metastatic indices for A549mock and A549KL were measured as the number of GFP colonies and RFP colonies, respectively. Also, 3LL cells were transplanted at the flanks of athymic mice by subcutaneous injection (2×10^6 cells per mouse) and treated with Klotho protein (0.01 mg/kg, intraperitoneal) or vehicle every other day for 10 days. Lungs were harvested 21 days after transplantation and the number of metastatic nodules was counted.

Cell Migration Assay—A549 cells stably transfected with a CMV-luciferase expression vector were incubated with or without TGF-β1 (2 ng/ml) or Klotho (5 nM) for 6 h and then transferred to Transwell chambers (20,000 cells per well). Cells migrating from the upper to lower chambers in 5 days were quantified by standard luciferase assays.

RESULTS

Recent studies demonstrated that forced expression of the *klotho* gene in extra-renal tissues mitigated decline of renal function in rodent models of chronic and acute renal failure (18, 31, 32), suggesting that the *klotho* gene product might function as a renoprotective factor in a non-cell-autonomous manner. To test a hypothesis that the secreted Klotho might mediate the renoprotective properties of the *klotho* gene, we investigated potential therapeutic effects of secreted Klotho on experimentally induced renal damage in mice.

UUO (obstruction of the right ureter by ligation) is a well-characterized experimental procedure that induces acute renal fibrosis in rodents (33). Ureteral obstruction induces hydronephrosis and results in renal fibrosis within a week. To determine whether Klotho protects kidneys from fibrosis induced by UUO, we administered purified recombinant secreted Klotho protein (0.01 mg/kg or 0.02 mg/kg) or vehicle into mice immediately after UUO by intraperitoneal injection followed by every other day injection and evaluated renal fibrosis 3 days and 7 days after UUO.

UUO induced progressive hydronephrosis as evidenced by enlargement of right renal pelvis in magnetic resonance imaging (MRI) analysis (Fig. 1*A*) (27). The average volume of pelvis was not different between Klotho-treated and vehicle-treated mice (Fig. 1*B*), indicating that Klotho treatment did not affect the severity of hydronephrosis induced by UUO. In contrast,

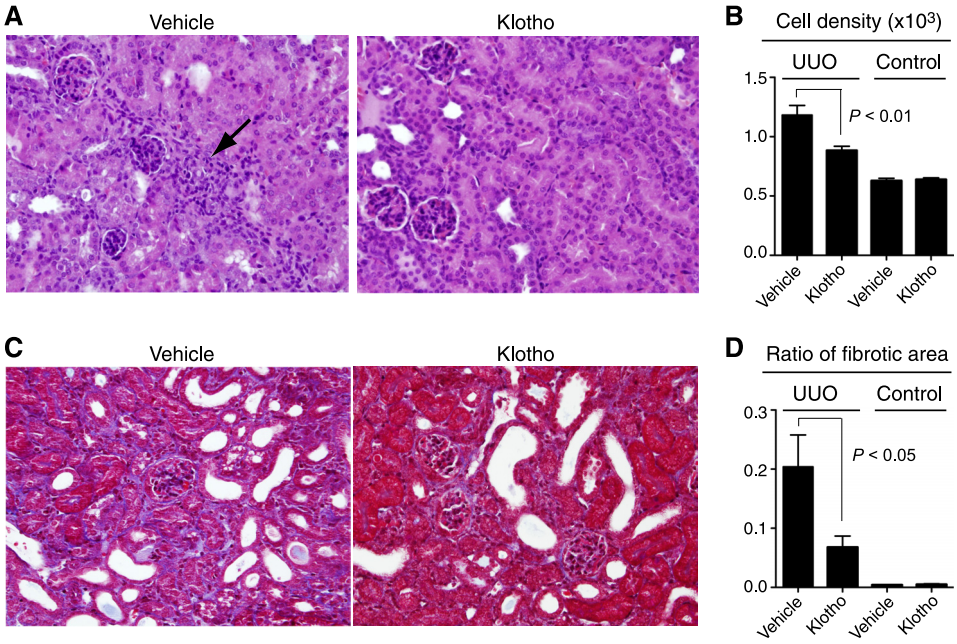

FIGURE 3. **Effects of Klotho protein injection on cell density and fibrosis in UUO mice determined by histological analysis.** *A*, typical histology of UUO kidneys from mice treated with vehicle or Klotho. Paraffin sections of UUO kidneys were stained with hematoxylin-eosin staining. The *arrow* indicates infiltration of myofibroblasts in the interstitial space. *B*, quantification of cell density. Five fields on a coronal section were selected randomly, and the number of nuclei in each field was counted under a high power field (original magnification ×400) by using the ImageJ software as described previously (27). Data indicate means ± S.E. $p < 0.01$ between the Vehicle-treated group ($n = 4$) and the Klotho-treated group ($n = 6$) in UUO kidneys by two-tailed *t* test. *C*, typical histology of UUO kidneys from mice treated with vehicle or Klotho. Paraffin sections of UUO kidneys were stained with Masson's trichrome that detected connective tissue as blue staining. *D*, Quantification of fibrotic area. Five fields on the coronal section were randomly selected and the ratios of blue to total areas in each field were counted in a high power field (original magnification ×400) using the ImageJ software. Data indicate means ± S.E. $p < 0.05$ between the vehicle-treated group ($n = 4$) and the Klotho-treated group ($n = 6$) in UUO kidneys by two-tailed *t* test.

the average volume of renal parenchyma in vehicle-treated mice was significantly smaller than that in Klotho-treated mice (Fig. 1, *A* and *B*), suggesting that Klotho treatment prevented parenchymal contraction associated with fibrosis. The contralateral non-obstructed left kidney did not exhibit significant changes in the pelvis and parenchymal volume (Fig. 1, *A* and *B*).

Another characteristic feature of UUO-induced renal fibrosis is infiltration of myofibroblasts into the interstitial space, which, in combination with contraction of the parenchymal volume, results in significant increase in parenchymal cell density. Increases in cell density and extracellular matrices associated with fibrosis restrict Brownian motion of water molecule in interstitial space that can be quantified by MRI as decreases in ADC (34). We reported that decrease in ADC was correlated with increase in cell density and expression levels of α-smooth muscle actin (αSMA), a marker for myofibroblasts, in UUO-induced renal fibrosis (27). The average ADC value in Klotho-treated mice was significantly higher than that in vehicle-treated mice (Fig. 2, *A* and *B*), indicating that Klotho treatment alleviated increases in cell density in renal parenchyma.

Consistent with the MRI findings, histological analysis confirmed that Klotho protein injection attenuated increases in cell density (Fig. 3, *A* and *B*) and connective tissues (Fig. 3, *C* and *D*). These observations suggest that Klotho protein injection is an effective treatment for renal fibrosis induced by UUO. Because UUO significantly reduced Klotho expression (Fig. 4*A*) and Klotho replacement therapy alleviated renal fibrosis, we conclude that reductions in renal Klotho expression contribute to pathogenesis of renal fibrosis.

To elucidate the molecular mechanism underlying the anti-fibrosis activity of Klotho, we asked if Klotho administration would alter expression of the genes involved in fibrogenic processes (23). We observed significant increase in expression of multiple mesenchymal markers in the UUO kidney, including αSMA (Fig. 4*B*, supplemental Fig. S1), collagen-1 (Fig. 4*C*, supplemental Fig. S2), Vimentin, and Matrix metallopeptidases (MMP-2, -3, -9) (supplemental Fig. S3) at the mRNA and/or protein levels. We also observed increased expression of Twist and Snail-1 (supplemental Fig. S3), transcription factors that transactivate these genes to confer mesenchymal phenotypes (35). Of note, induction of Snail-1 expression was sufficient to induce renal fibrosis in mice (36). Klotho treatment attenuated induction of Snail-1, as well as all these mesenchymal markers (Fig. 4, *B* and *C*, supplemental Figs. S1–S3).

Because Snail-1 expression is primarily induced by TGF-β1 (37), we speculated that Klotho might suppress UUO-induced increases in TGF-β1 expression in kidney. However, it was not the case (Fig. 4*D*). Expression of other inflammatory cytokines, including IL-1α and TNF-α, were not suppressed, either (data not shown). These observations suggest that secreted Klotho does not reduce TGF-β1 expression through alleviating inflammatory responses, in general, but may specifically inhibit TGF-β1 signaling.

To test this possibility, we stimulated cultured renal epithelial cells (NRK52E) with TGF-β1 in the presence or absence of secreted Klotho protein and asked if Klotho might inhibit the canonical TGF-β1 signaling pathway. TGF-β1 signaling is mediated by two types of receptor serine-threonine kinases

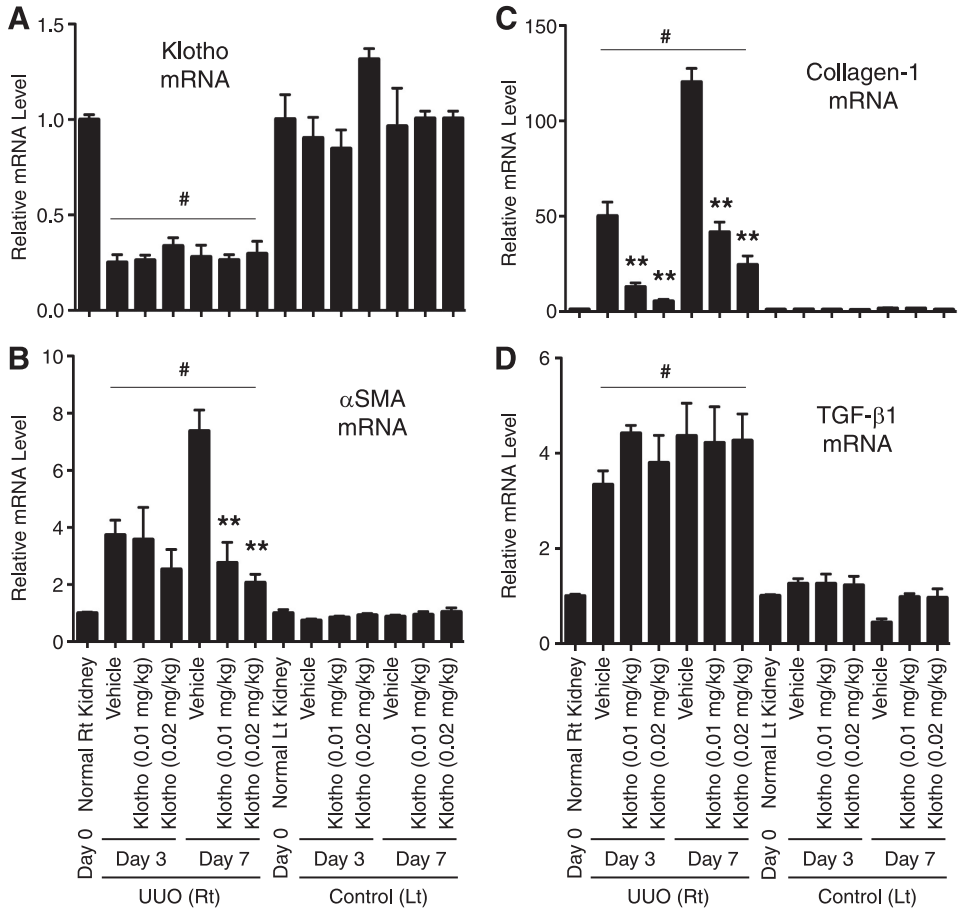

FIGURE 4. **Klotho protein injection suppresses mesenchymal marker expression in UUO kidney.** *A*, Klotho mRNA levels determined by quantitative RT-PCR (qPCR). Right kidneys (UUO) and left kidneys (Control) from mice treated with vehicle ($n = 5$) and Klotho (0.01 mg/kg or 0.02 mg/kg, $n = 5$ for each dose) were compared on Day 3 and Day 7. Expression levels of mRNA were normalized with those in normal kidneys (Day 0). Data indicate means ± S.E. *, $p < 0.05$; **, $p < 0.01$ *versus* vehicle-treated mice at the same time points by two-tailed *t* test. #, $p < 0.05$ *versus* mice at Day 0 by two-tailed *t* test. *B*, αSMA mRNA levels. *C*, collagen-1 mRNA levels. *D*, TGF-β1 mRNA levels.

(38). Binding of TGF-β1 to the type-II receptor (TGFβR2) recruits and activates the type-I receptor (TGFβR1) that phosphorylates Smad2/3. Phosphorylated Smad2/3 translocates into the nucleus and functions as a transcription factor to regulate expression of TGF-β1 target genes. Klotho inhibited TGF-β1-induced phosphorylation of Smad2 in a dose-dependent manner in NRK52E cells (Fig. 5*A*) and transactivation of a Smad-responsive reporter in HEK293 human embryonic kidney cells (Fig. 5*B*) and in NRK52E cells (supplemental Fig. S5). Klotho also suppressed TGF-β1-induced increases in αSMA (Fig. 5*C*) and Vimentin (Fig. 5*D*) expression in cultured renal epithelial cells.

As a potential molecular mechanism by which secreted Klotho inhibits TGF-β1 signaling, we identified direct protein-protein interaction between Klotho and the TGFβR2 (Fig. 6*A*). The apparent dissociation constant (K_d) of Klotho and TGF-β1 to TGFβR2 *in vitro* was 1.9 nM and 0.77 nM, respectively. We previously identified high affinity binding of Klotho to fibroblast growth factor receptor (FGFR) 1c (K_d = 72 nM) (39). Although binding of Klotho to FGFR1c significantly enhanced the affinity of FGFR1c to a particular FGF ligand (FGF23) (6, 7), binding of Klotho to TGFβR2 significantly reduced TGF-β1 binding to TGFβR2 *in vitro* (Fig. 6*B*), as well as to the surface of cultured renal epithelial cells (Fig. 6*C*) and lung epithelial cells (supplemental Fig. S6), which explains the ability of Klotho to inhibit TGF-β1 signaling. In addition, the ability of Klotho to inhibit TGF-β1-induced activation of Smad-sensitive reporter activity was slightly attenuated or completely abolished by overexpression of TGFβR2 or constitutive-active TGFβR1, respectively (supplemental Fig. S5), further confirming that Klotho acts to abrogate TGFβR2 function. It remains to be determined whether Klotho inhibits TGF-β1 binding in a competitive or allosteric manner.

Because inhibition of TGF-β1 activity by administration of neutralizing antibody for TGF-β1 mitigated UUO-induced renal fibrosis (25), we hypothesized that the anti-fibrosis activity of secreted Klotho protein might be attributed to its ability to inhibit TGF-β1 signaling, at least in part. To support this hypothesis, we treated UUO mice with the TGF-β1 antibody alone or Klotho protein alone or both in combination, and asked if the combination treatment would exert additive therapeutic benefits when compared with individual treatments. Effects of the TGF-β1 antibody treatment on expression of mesenchymal markers were comparable with those of the Klotho protein treatment. The combination treatment with the TGF-β1 antibody and Klotho protein did not induce further suppression of mesenchymal marker expression (Fig. 7), which did not contradict the notion that TGF-β1 antibody and Klotho

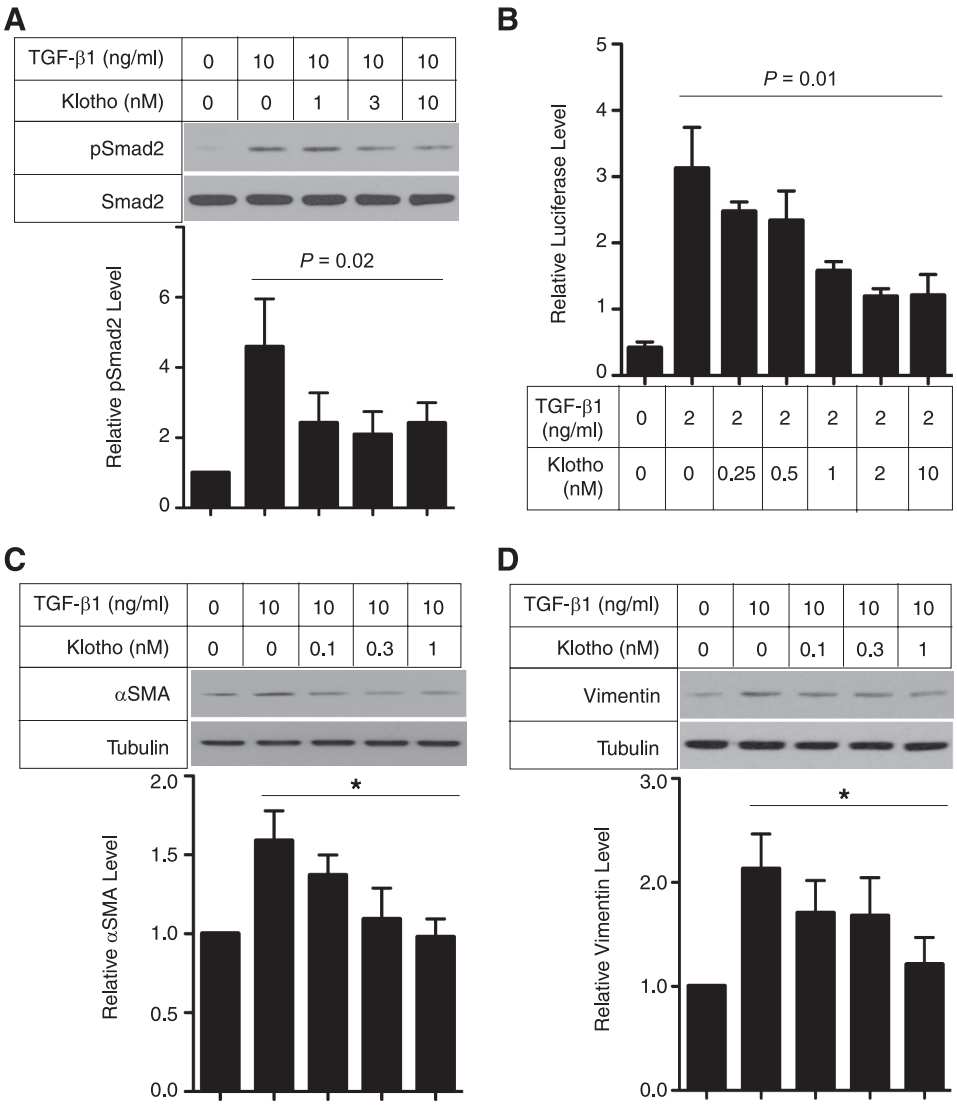

FIGURE 5. **Klotho protein inhibits TGF-β1 signaling and suppresses expression of mesenchymal markers in cultured cells.** *A*, Klotho inhibits TGF-β1-induced phosphorylation of Smad2. NRK52E renal epithelial cells were incubated with secreted Klotho protein at the indicated doses for 30 min and then stimulated with TGF-β1 (10 ng/ml) for 30 min. Cell lysates were subjected to immunoblot analysis using antibody against phosphorylated Smad2 (pSmad2) or antibody that recognized Smad2 regardless of its phosphorylation state (Smad2). Typical results of 5 independent experiments are shown (*upper panel*). pSmad2/Smad2 ratios in each treatment were normalized with those without TGF-β1 and Klotho. Data indicate means ± S.E. of five independent experiments (*lower panel*). $p = 0.02$ by one-way ANOVA. *B*, Klotho inhibits TGF-β1-induced activation of a Smad-responsive reporter. HEK293 cells were transfected with a luciferase reporter containing Smad response elements (pGTCT2 × 2-Luc) and a lacZ expression vector for normalization. These cells were incubated with TGF-β1 and/or Klotho at the indicated doses and subjected to standard luciferase assays. Data indicate means ± S.E. of three independent experiments. $p = 0.01$ by one-way ANOVA. *C*, Klotho suppresses TGF-β1-induced increase in α-smooth muscle actin (αSMA) protein. NRK52E cells were incubated with Klotho protein and TGF-β1 at the indicated doses for 48 h in DMEM supplemented with 1% FBS. Cell lysates were subjected to immunoblot analysis using antibodies against αSMA and tubulin. A typical result of five independent experiments was shown (*upper panel*). The αSMA/tubulin ratios in each treatment were normalized with those without treatment. Data indicate means ± S.E. of five independent experiments (*lower panel*). *, $p < 0.01$ by one-way ANOVA. *D*, same as *C*, except that anti-Vimentin antibody was used.

might suppress renal fibrosis by a common mechanism, namely, by preventing TGF-β1 from binding to TGFβR2.

TGF-β1-mediated mesenchymal transition plays a critical role not only in tissue fibrosis, but also in cancer metastasis (21). Once cancer cells undergo EMT, they acquire the ability to migrate from the primary lesion and invade into neighboring tissues and blood vessels, leading to formation of metastatic lesions.

To verify potential anti-metastasis activity of Klotho, we first tested whether forced expression of Klotho in cancer cells might suppress metastasis in mice with cancer xenografts. A human lung cancer cell line, A549, was stably transfected with an expression vector for membrane Klotho protein or a mock vector. Klotho-transfected cells released Klotho ectodomain (secreted Klotho protein) into conditioned medium (supplemental Fig. S4). Cell lines that showed no difference in cell cycle distribution, growth rates, and plating efficiency in culture were selected and transplanted into athymic mice by tail vein injection. Mice injected with Klotho-expressing A549 cells (A549KL) survived significantly longer than those injected with an equal number of mock-transfected cells (A549mock) (Fig. 8*A*). Consistent with the improved survival, A549KL cells generated less metastasis than A549mock cells (Fig. 8*B*). Also, A549KL cells exhibited

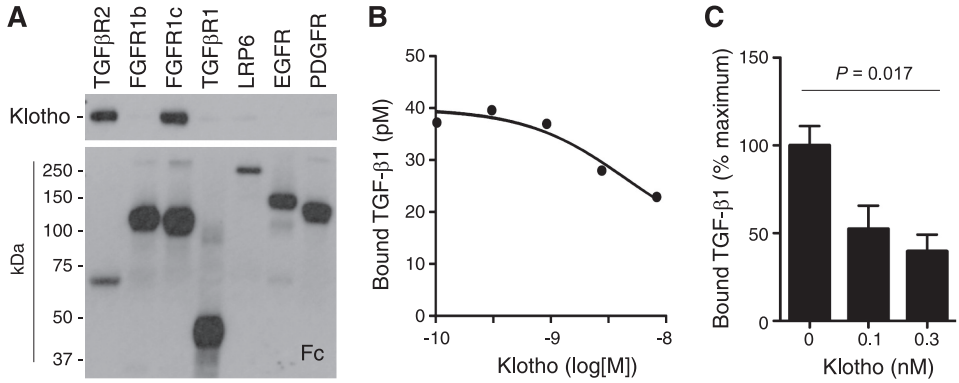

FIGURE 6. **Klotho binds to TGFβR2 and inhibits TGF-β1 binding to the receptor.** *A*, direct protein-protein interaction between Klotho and TGFβR2. Klotho protein was incubated with recombinant receptor ectodomain proteins with a human Fc tag and pulled down with protein A beads. The beads-bound protein was detected by immunoblot analysis using anti-Klotho (*upper panel*) or anti-human IgG (Fc, *lower panel*) antibodies. TGFβR2; Type-II TGF-β receptor, FGFR1b; fibroblast growth factor receptor 1α (IIIb), FGFR1c; fibroblast growth factor receptor 1α (IIIc), TGFβR1; Type-I TGF-β receptor, LRP-6; LDL receptor-related protein 6, EGFR; epidermal growth factor receptor, PDGFR; platelet-derived growth factor receptor-α. Klotho was reported to bind to FGFR1c but not to FGFR1b (6, 39), which served as positive and negative controls, respectively. *B*, Klotho inhibits TGF-β1 binding to TGFβR2 *in vitro*. TGF-β1 binding assays were performed using recombinant TGFβR2 protein on protein A beads in the presence of Klotho protein. Data indicate means of duplicated measurement and a fitting curve ($R^2 = 0.776$). *C*, Klotho inhibits TGF-β1 binding to renal epithelial cells. TGF-β1 binding assay was performed in NRK52E cells in the presence of Klotho protein. Data indicate means ± S.E. ($n = 4$ for each dose). $p = 0.017$ by one-way ANOVA.

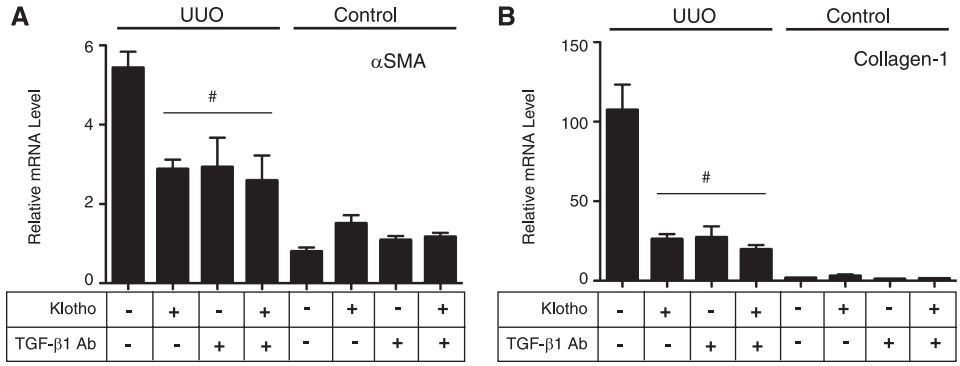

FIGURE 7. **Minimal additive effect of Klotho protein and neutralizing TGF-β1 antibody on mesenchymal marker expression in UUO kidney.** UUO mice were treated with Klotho (0.02 mg/kg, intraperitoneal) or TGF-β1 antibody (1.5 mg/kg, intraperitoneal) or both every 48 h. On Day 7, mRNA levels of αSMA and collagen-1 in the right (UUO) and left (Control) kidneys were determined by qPCR. Data indicate means ± S.E. #, $p < 0.05$ *versus* mice without treatment by two-tailed *t* test.

attenuation of Smad3 phosphorylation induced by TGF-β1 (supplemental Fig. S4*B*).

To determine whether the inhibitory effect of Klotho on cancer metastasis was cell-autonomous, we next asked if transgenic mice that overexpressed Klotho (1, 2) would survive cancer transplantation longer than wild-type mice. For this purpose we used another human cancer cell line, 3LL (Lewis Lung cancer), which is an aggressive cell line that can proliferate and metastasize in syngeneic mice when injected in tail vein or via subcutaneous injections. Transplantation of 3LL cells killed all the wild-type mice within 25 days. In contrast, 40% of Klotho-overexpressing transgenic mice survived beyond 25 days (Fig. 8*C*), indicating that the anti-metastasis activity of Klotho may be non-cell-autonomous and possibly mediated by secreted Klotho.

Lastly, we tested whether injection of secreted Klotho protein would suppress cancer metastasis. Wild-type mice were exposed to 3LL cells by intravenous injection and then treated with secreted Klotho protein (0.01 mg/kg) or vehicle in the same way as we did for UUO mice. Klotho-treated mice survived significantly longer than vehicle-treated mice (Fig. 8*D*). To further confirm that Klotho treatment reduced metastasis, we transplanted 3LL cells into athymic mice at flank regions by subcutaneous injection and then treated them with vehicle or secreted Klotho protein. Klotho-treated mice generated fewer metastatic nodules in the lung than vehicle-treated mice (Fig. 8*E*).

Consistent with these findings *in vivo*, secreted Klotho protein inhibited TGF-β1 signaling and suppressed EMT in cultured A549 cells. Klotho inhibited TGF-β1-induced phosphorylation of Smad3 (Fig. 9*A*), transactivation of the Smad-responsive reporter (Fig. 9*B*), and binding of TGF-β1 to the cell surface (Fig. 9*C*) in a dose-dependent manner, as observed in renal epithelial cells (Fig. 5). TGF-β1 treatment caused decreased epithelial marker expression (E-cadherin), increased mesenchymal marker expression (N-cadherin) (Fig. 9*D*), and increased migration of A549 cells (Fig. 9*E*). All these TGF-β1-induced EMT responses were attenuated by adding secreted Klotho protein to the medium.

DISCUSSION

We have demonstrated that secreted Klotho suppresses renal fibrosis induced by UUO (Figs. 1–4, supplemental Figs. S1–S3) and cancer metastasis in mice transplanted with human cancer

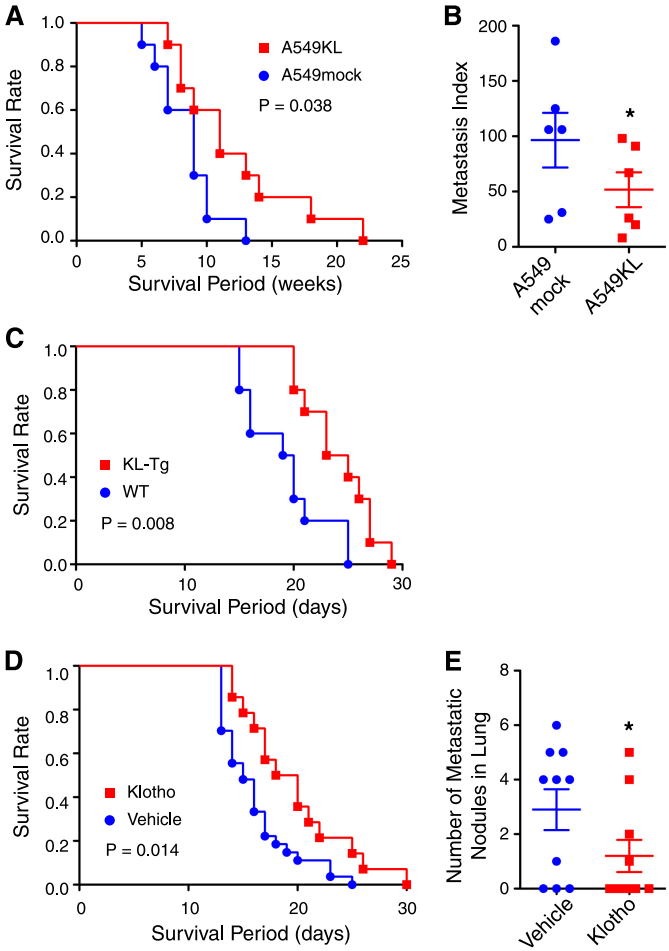

FIGURE 8. **Klotho suppresses cancer metastasis and improve survival in mice.** *A*, mice transplanted with A549KL cells ($n = 10$) survived longer than those transplanted with A549mock cells ($n = 10$). $p = 0.038$ by log-rank test. *B*, A549KL cells metastasize to the lung less efficiently than A549mock cells. A549KL and A549mock cells were labeled with different colors (GFP or RFP), mixed at 1:1 ratio, and transplanted into athymic mice ($n = 6$) by tail vein injection. Cells colonized in the lung were quantified by counting the number of colonies grown from the lung primary culture (metastatic index). Data indicate means ± S.E. *, $p < 0.05$ by two-tailed *t* test. *C*, Klotho-overexpressing transgenic mice (*KL-Tg*, $n = 10$) survived the 3LL transplantation longer than wild-type mice (WT, $n = 10$). $p = 0.008$ by log-rank test. *D*, Klotho protein injection improved survival of 3LL-transplanted mice. Wild-type mice were transplanted with 3LL cells by tail vein injection and then treated with Klotho protein (0.01 mg/kg, every 48 h, $n = 14$) or vehicle ($n = 27$). $p = 0.014$ by log-rank test. *E*, athymic nude mice were transplanted with 3LL cells by subcutaneous injection and then treated with Klotho protein (0.01 mg/kg, intraperitoneal, every 48 h, $n = 10$) or vehicle ($n = 10$) for 10 days. Lungs were harvested 3 weeks after transplantation to count the number of metastatic nodules. *, $p < 0.05$ by one-tailed *t* test with Welch's correction.

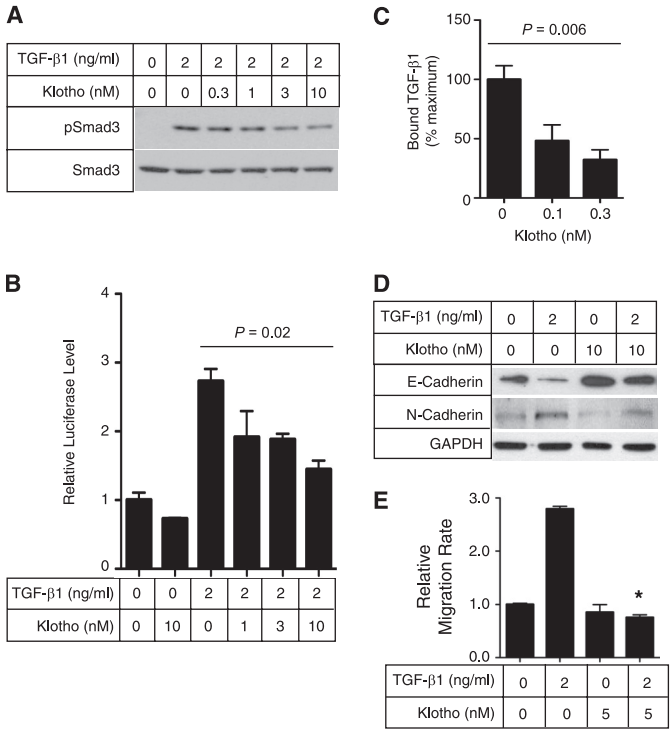

FIGURE 9. **Secreted Klotho inhibits EMT in A549 cancer cells.** *A*, Klotho inhibits TGF-β1-induced phosphorylation of Smad3 in A549 cells. A549 cells were incubated with secreted Klotho protein for 15 min and then stimulated with TGF-β1 for 15 min at the indicated doses. Cell lysates were subjected to immunoblot analyses using antibody against phosphorylated Smad3 (*pSmad3*) or antibody that recognized Smad3 regardless of its phosphorylation state (*Smad3*). *B*, Klotho inhibits TGF-β1-induced activation of the Smad-responsive reporter. A549 cells were transfected with a luciferase reporter containing Smad response elements (pGTCT2 × 2-Luc) and a lacZ expression vector for normalization. These cells were incubated with TGF-β1 or Klotho at the indicated doses for 6 h and subjected to a standard luciferase assay. The luciferase activity was normalized with that of non-treated cells. Data indicate means ± S.E. of three independent experiments. $p = 0.02$ by one-way ANOVA. *C*, Klotho inhibits TGF-β1 binding to A549 cells. TGF-β1 binding assays were performed in A549 cells in the absence or presence of Klotho protein (0.1 or 0.3 nM). The amount of bound TGF-β1 was normalized with that without Klotho. Data indicate means ± S.E. of four independent experiments. $p = 0.006$ by one-way ANOVA. *D*, Klotho protein suppresses TGF-β1-induced decrease in E-cadherin and increase in N-cadherin. A549 cells were treated with TGF-β1 and/or Klotho at the indicated doses for 6 h and then subjected to immunoblot analyses 48 h later. *E*, Klotho protein suppresses TGF-β1-induced cell migration. A549 cells were treated with TGF-β1 and/or Klotho at the indicated doses for 6 h and then subjected to a standard Transwell migration assay. Data indicate means ± S.E. of three independent experiments. *, $p < 0.001$ *versus* TGF-β1 treatment alone by two-tailed *t* test.

cells (Fig. 8). As a potential mechanism, we identified a novel activity of Klotho that inhibits TGF-β1 signaling (Figs. 5, *A* and *B* and 9, *A* and *B*, & supplemental Fig. S5) and EMT responses both *in vitro* (Fig. 5, *C* and *D* and 9, *D* and *E*, & supplemental Fig. S4) and *in vivo* (Fig. 4 & supplemental Fig. S3). Secreted Klotho binds to TGFβR2 and inhibits binding of TGF-β1 both in test tubes (Fig. 6, *A* and *B*) and in cultured cells (Figs. 6*C* and 9*C* and supplemental Figs. S5 and S6). Because TGF-β1 has been implicated as a "master switch" of EMT in various types of cells and because EMT plays a critical role both in tissue fibrosis and in cancer metastasis (22), the present study has raised the possibility that the ability of secreted Klotho to inhibit TGF-β1 signaling may contribute to the therapeutic effects of Klotho on renal fibrosis and cancer metastasis, at least in part. Lack of additive effects of Klotho and anti-TGF-β1 antibody on EMT *in vivo* (Fig. 7) indirectly supports this hypothesis. However, secreted Klotho inhibits not only TGF-β1 but also Wnt (16) and IGF-1 signaling (1, 17) that can all contribute to the promotion of EMT. Thus, it is likely that the anti-EMT properties of Klotho may be attributed to its ability to inhibit TGF-β1, Wnt, and IGF-1 signaling pathways simultaneously. Further studies are necessary to determine which activity of Klotho contributes most significantly to the therapeutic effects of secreted Klotho on renal fibrosis and caner metastasis.

Renal fibrosis is a final common pathology of chronic kidney disease (CKD). More than 26 million Americans, or 13% total population, has CKD and is increasingly recognized as a global

public health problem (40). CKD is associated with marked decrease in renal Klotho expression (41). These observations and the present study justify urgent need for pre-clinical and clinical studies to test whether Klotho deficiency may contribute to pathogenesis of renal fibrosis in CKD and that Klotho replacement therapy may be effective for CKD-induced renal fibrosis as well.

The present study used MRI as a non-invasive method for evaluating renal fibrosis in mice. This is because MRI, unlike computed tomography (CT), can detect and quantify fibrosis-associated changes at the histological and functional level. ADC determined by MRI reflects cell density in renal parenchyma, which correlates the degree of fibrosis and mesenchymal marker expression as shown in our previous (27) and present studies. Also, decreased ADC is associated with decreased glomerular filtration rate (42), suggesting that ADC measurement allows evaluation of functional difference between the right or left kidney. In addition, MRI is free from ionizing irradiation. Currently, MRI is not regarded as a standard diagnostic tool for renal fibrosis in humans. However, these advantages of MRI over CT may justify further validation of renal ADC as a biomarker for monitoring presence, progression, and response to therapy in human renal fibrosis.

Several studies have identified association between Klotho and cancer in humans. Decreased Klotho expression is associated with invasive breast cancer (17) and cervical cancer (43). These studies observed loss of Klotho expression primarily in invasive carcinoma, but not in carcinoma *in situ* or the early non-invasive phase, suggesting that Klotho may be involved not in cancer initiation but in cancer metastasis. These findings coincide with the fact that Klotho counteracts EMT, and imply that adverse effects of decreased Klotho on cancer may be enhanced in a population with accelerated cancer initiation. In fact, a functional variation of Klotho (F352V/C370S) that exhibits reduced secretion in *in vitro* experiments (44) is associated with increased risk for breast and ovarian cancer as well as with younger age at diagnosis among BRCA1 mutation carriers (45). Because inhibition of IGF-1 receptor suppresses breast cancer (46), these observations have been explained by the ability of Klotho to suppress IGF-1 signaling (1, 17). The present study has raised the possibility that the ability of Klotho to suppress TGF-β1 signaling may also partly contribute to the anti-cancer properties of Klotho.

Although we have shown a novel activity of secreted Klotho that inhibits TGF-β1 signaling, we have not excluded the possibility that the activity of secreted Klotho that inhibits IGF-1 (1, 17) and Wnt (16) signaling pathways may also contribute to the therapeutic effects of secreted Klotho on renal fibrosis and cancer metastasis. Because Wnt can also function as a mediator of mesenchymal transition, we tested whether inhibition of Wnt signaling contributed to the therapeutic effect of secreted Klotho protein on renal fibrosis. We introduced renal fibrosis by UUO in TOPGAL mice, which carried a transgene that expressed β-galactosidase in response to activation of the canonical Wnt signaling pathway (47), and treated them with Klotho protein (0.02 mg/kg, intraperitoneal, every other day) or vehicle for 7 days. We were unable to detect significant decrease in β-galactosidase activity by the Klotho treatment in the UUO kidneys (data not shown). Together with the finding that combination therapy of secreted Klotho and TGF-β1 neutralizing antibody did not exhibit significant additive benefits (Fig. 7), we speculate that contribution of TGF-β1 signaling inhibition may be more significant than that of Wnt signaling inhibition to the therapeutic effects of secreted Klotho on UUO-induced renal fibrosis. Additional studies are needed to make a more definitive conclusion whether or not the ability of Klotho to inhibit TGF-β1 signaling contributes to its anti-EMT properties.

IGF-1, Wnt, and TGF-β1 signaling pathways have been targets of therapeutic interventions in various types of tissue fibrosis and/or cancer. Secreted Klotho protein is unique in that it can inhibit these three signaling pathways simultaneously. This unique feature of secreted Klotho protein can be a major advantage over numerous individual inhibitors in clinical and pre-clinical development, including IGF-1 receptor antibodies, tyrosine kinase inhibitors (48), Wnt signaling inhibitors (49), TGF-β1 neutralizing antibodies, soluble TGFβR2, and TGF-β receptor kinase inhibitors (50, 51). In addition, Klotho therapy will be safe, since Klotho overexpression extends life span in mice (1). We suggest that secreted Klotho protein may be a novel therapeutic reagent for tissue fibrosis and cancer metastasis with unique mechanism of action.

Acknowledgments—We thank John M. Shelton and James A. Richardson for help with histological analyses.

REFERENCES

1. Kurosu, H., Yamamoto, M., Clark, J. D., Pastor, J. V., Nandi, A., Gurnani, P., McGuinness, O. P., Chikuda, H., Yamaguchi, M., Kawaguchi, H., Shimomura, I., Takayama, Y., Herz, J., Kahn, C. R., Rosenblatt, K. P., and Kuro-o, M. (2005) *Science* **309,** 1829–1833
2. Kuro-o, M., Matsumura, Y., Aizawa, H., Kawaguchi, H., Suga, T., Utsugi, T., Ohyama, Y., Kurabayashi, M., Kaname, T., Kume, E., Iwasaki, H., Iida, A., Shiraki-Iida, T., Nishikawa, S., Nagai, R., and Nabeshima, Y. I. (1997) *Nature* **390,** 45–51
3. Imura, A., Iwano, A., Tohyama, O., Tsuji, Y., Nozaki, K., Hashimoto, N., Fujimori, T., and Nabeshima, Y. (2004) *FEBS Lett.* **565,** 143–147
4. Chen, C. D., Podvin, S., Gillespie, E., Leeman, S. E., and Abraham, C. R. (2007) *Proc. Natl. Acad. Sci. U.S.A.* **104,** 19796–19801
5. Bloch, L., Sineshchekova, O., Reichenbach, D., Reiss, K., Saftig, P., Kuro-o, M., and Kaether, C. (2009) *FEBS Lett.* **583,** 3221–3224
6. Kurosu, H., Ogawa, Y., Miyoshi, M., Yamamoto, M., Nandi, A., Rosenblatt, K. P., Baum, M. G., Schiavi, S., Hu, M. C., Moe, O. W., and Kuro-o, M. (2006) *J. Biol. Chem.* **281,** 6120–6123
7. Urakawa, I., Yamazaki, Y., Shimada, T., Iijima, K., Hasegawa, H., Okawa, K., Fujita, T., Fukumoto, S., and Yamashita, T. (2006) *Nature* **444,** 770–774
8. White, K. E., Evans, W. E., O'Rlordan, J. L. H., Speer, M. C., Econs, M. J., Lorenz-Deplereux, B., Grabowski, M., Meitinger, T., and Storm, T. M. (2000) *Nat. Genet.* **26,** 345–348
9. Shimada, T., Hasegawa, H., Yamazaki, Y., Muto, T., Hino, R., Takeuchi, Y., Fujita, T., Nakahara, K., Fukumoto, S., and Yamashita, T. (2004) *J. Bone Miner. Res.* **19,** 429–435
10. Yu, X., Ibrahimi, O. A., Goetz, R., Zhang, F., Davis, S. I., Garringer, H. J., Linhardt, R. J., Ornitz, D. M., Mohammadi, M., and White, K. E. (2005) *Endocrinology* **146,** 4647–4656
11. Goetz, R., Beenken, A., Ibrahimi, O. A., Kalinina, J., Olsen, S. K., Eliseenkova, A. V., Xu, C., Neubert, T. A., Zhang, F., Linhardt, R. J., Yu, X., White, K. E., Inagaki, T., Kliewer, S. A., Yamamoto, M., Kurosu, H., Ogawa, Y., Kuro-o, M., Lanske, B., Razzaque, M. S., and Mohammadi, M. (2007) *Mol. Cell Biol.* **27,** 3417–3428

12. Chang, Q., Hoefs, S., van der Kemp, A. W., Topala, C. N., Bindels, R. J., and Hoenderop, J. G. (2005) *Science* **310,** 490–493
13. Cha, S. K., Ortega, B., Kurosu, H., Rosenblatt, K. P., Kuro-o, M., and Huang, C. L. (2008) *Proc. Natl. Acad. Sci. U.S.A.* **105,** 9805–9810
14. Cha, S. K., Hu, M. C., Kurosu, H., Kuro-o, M., Moe, O., and Huang, C. L. (2009) *Mol. Pharmacol.* **76,** 38–46
15. Hu, M. C., Shi, M., Zhang, J., Pastor, J., Nakatani, T., Lanske, B., Razzaque, M. S., Rosenblatt, K. P., Baum, M. G., Kuro-o, M., and Moe, O. W. (2010) *FASEB J.* **24,** 3438–3450
16. Liu, H., Fergusson, M. M., Castilho, R. M., Liu, J., Cao, L., Chen, J., Malide, D., Rovira, II, Schimel, D., Kuo, C. J., Gutkind, J. S., Hwang, P. M., and Finkel, T. (2007) *Science* **317,** 803–806
17. Wolf, I., Levanon-Cohen, S., Bose, S., Ligumsky, H., Sredni, B., Kanety, H., Kuro-o, M., Karlan, B., Kaufman, B., Koeffler, H. P., and Rubinek, T. (2008) *Oncogene* **27,** 7094–7105
18. Haruna, Y., Kashihara, N., Satoh, M., Tomita, N., Namikoshi, T., Sasaki, T., Fujimori, T., Xie, P., and Kanwar, Y. S. (2007) *Proc. Natl. Acad. Sci. U.S.A.* **104,** 2331–2336
19. Iwano, M., Plieth, D., Danoff, T. M., Xue, C., Okada, H., and Neilson, E. G. (2002) *J. Clin. Invest.* **110,** 341–350
20. Humphreys, B. D., Lin, S. L., Kobayashi, A., Hudson, T. E., Nowlin, B. T., Bonventre, J. V., Valerius, M. T., McMahon, A. P., and Duffield, J. S. (2010) *Am. J. Pathol.* **176,** 85–97
21. Thiery, J. P., Acloque, H., Huang, R. Y., and Nieto, M. A. (2009) *Cell* **139,** 871–890
22. Willis, B. C., and Borok, Z. (2007) *Am. J. Physiol. Lung Cell Mol. Physiol.* **293,** L525–534
23. Zeisberg, M., and Neilson, E. G. (2009) *J. Clin. Invest.* **119,** 1429–1437
24. Ling, H., Li, X., Jha, S., Wang, W., Karetskaya, L., Pratt, B., and Ledbetter, S. (2003) *J. Am. Soc. Nephrol.* **14,** 377–388
25. El Chaar, M., Chen, J., Seshan, S. V., Jha, S., Richardson, I., Ledbetter, S. R., Vaughan, E. D., Jr., Poppas, D. P., and Felsen, D. (2007) *Am. J. Physiol. Renal Physiol.* **292,** F1291–F1301
26. Ganapathy, V., Ge, R., Grazioli, A., Xie, W., Banach-Petrosky, W., Kang, Y., Lonning, S., McPherson, J., Yingling, J. M., Biswas, S., Mundy, G. R., and Reiss, M. (2010) *Mol. Cancer* **9,** 122
27. Togao, O., Doi, S., Kuro-o, M., Masaki, T., Yorioka, N., and Takahashi, M. (2010) *Radiology* **255,** 772–780
28. Kawai, T., Masaki, T., Doi, S., Arakawa, T., Yokoyama, Y., Doi, T., Kohno, N., and Yorioka, N. (2009) *Lab. Invest.* **89,** 47–58
29. Kurosu, H., Choi, M., Ogawa, Y., Dickson, A. S., Goetz, R., Eliseenkova, A. V., Mohammadi, M., Rosenblatt, K. P., Kliewer, S. A., and Kuro-o, M. (2007) *J. Biol. Chem.* **282,** 26687–26695
30. Kato, Y., Arakawa, E., Kinoshita, S., Shirai, A., Furuya, A., Yamano, K., Nakamura, K., Iida, A., Anazawa, H., Koh, N., Iwano, A., Imura, A., Fujimori, T., Kuro-o, M., Hanai, N., Takeshige, K., and Nabeshima, Y. (2000) *Biochem. Biophys. Res. Commun.* **267,** 597–602
31. Sugiura, H., Yoshida, T., Tsuchiya, K., Mitobe, M., Nishimura, S., Shirota, S., Akiba, T., and Nihei, H. (2005) *Nephrol. Dial Transplant* **20,** 2636–2645
32. Mitani, H., Ishizaka, N., Aizawa, T., Ohno, M., Usui, S., Suzuki, T., Amaki, T., Mori, I., Nakamura, Y., Sato, M., Nangaku, M., Hirata, Y., and Nagai, R. (2002) *Hypertension* **39,** 838–843
33. Klahr, S., and Morrissey, J. (2002) *Am. J. Physiol. Renal Physiol* **283,** F861–875
34. Lyng, H., Haraldseth, O., and Rofstad, E. K. (2000) *Magn. Reson. Med.* **43,** 828–836
35. Acloque, H., Adams, M. S., Fishwick, K., Bronner-Fraser, M., and Nieto, M. A. (2009) *J. Clin. Invest.* **119,** 1438–1449
36. Boutet, A., De Frutos, C. A., Maxwell, P. H., Mayol, M. J., Romero, J., and Nieto, M. A. (2006) *EMBO J.* **25,** 5603–5613
37. Peinado, H., Quintanilla, M., and Cano, A. (2003) *J. Biol. Chem.* **278,** 21113–21123
38. Feng, X. H., and Derynck, R. (2005) *Annu. Rev. Cell Dev. Biol.* **21,** 659–693
39. Goetz, R., Nakada, Y., Hu, M. C., Kurosu, H., Wang, L., Nakatani, T., Shi, M., Eliseenkova, A. V., Razzaque, M. S., Moe, O. W., Kuro-o, M., and Mohammadi, M. (2010) *Proc. Natl. Acad. Sci. U.S.A.* **107,** 407–412
40. Coresh, J., Selvin, E., Stevens, L. A., Manzi, J., Kusek, J. W., Eggers, P., Van Lente, F., and Levey, A. S. (2007) *JAMA* **298,** 2038–2047
41. Koh, N., Fujimori, T., Nishiguchi, S., Tamori, A., Shiomi, S., Nakatani, T., Sugimura, K., Kishimoto, T., Kinoshita, S., Kuroki, T., and Nabeshima, Y. (2001) *Biochem. Biophys. Res. Commun.* **280,** 1015–1020
42. Xu, Y., Wang, X., and Jiang, X. (2007) *J. Magn. Reson. Imaging* **26,** 678–681
43. Lee, J., Jeong, D. J., Kim, J., Lee, S., Park, J. H., Chang, B., Jung, S. I., Yi, L., Han, Y., Yang, Y., Kim, K. I., Lim, J. S., Yang, I., Jeon, S., Bae, D. H., Kim, C. J., and Lee, M. S. (2010) *Mol. Cancer* **9,** 109
44. Arking, D. E., Krebsova, A., Macek, M., Sr., Macek, M., Jr., Arking, A., Mian, I. S., Fried, L., Hamosh, A., Dey, S., McIntosh, I., and Dietz, H. C. (2002) *Proc. Natl. Acad. Sci. U.S.A.* **99,** 856–861
45. Wolf, I., Laitman, Y., Rubinek, T., Abramovitz, L., Novikov, I., Beeri, R., Kuro-o, M., Koeffler, H. P., Catane, R., Freedman, L. S., Levy-Lahad, E., Karlan, B. Y., Friedman, E., and Kaufman, B. (2010) *Oncogene* **29,** 26–33
46. Mitsiades, C. S., Mitsiades, N. S., McMullan, C. J., Poulaki, V., Shringarpure, R., Akiyama, M., Hideshima, T., Chauhan, D., Joseph, M., Libermann, T. A., García-Echeverría, C., Pearson, M. A., Hofmann, F., Anderson, K. C., and Kung, A. L. (2004) *Cancer Cell* **5,** 221–230
47. DasGupta, R., and Fuchs, E. (1999) *Development* **126,** 4557–4568
48. Weroha, S. J., and Haluska, P. (2008) *J. Mammary Gland Biol. Neoplasia* **13,** 471–483
49. Huang, S. M., Mishina, Y. M., Liu, S., Cheung, A., Stegmeier, F., Michaud, G. A., Charlat, O., Wiellette, E., Zhang, Y., Wiessner, S., Hild, M., Shi, X., Wilson, C. J., Mickanin, C., Myer, V., Fazal, A., Tomlinson, R., Serluca, F., Shao, W., Cheng, H., Shultz, M., Rau, C., Schirle, M., Schlegl, J., Ghidelli, S., Fawell, S., Lu, C., Curtis, D., Kirschner, M. W., Lengauer, C., Finan, P. M., Tallarico, J. A., Bouwmeester, T., Porter, J. A., Bauer, A., and Cong, F. (2009) *Nature* **461,** 614–620
50. Yingling, J. M., Blanchard, K. L., and Sawyer, J. S. (2004) *Nat. Rev. Drug Discov.* **3,** 1011–1022
51. Prud'homme, G. J. (2007) *Lab. Invest.* **87,** 1077–1091